Songklanakarin J. Sci. Technol.
46 (3), 316–322, May – Jun. 2024

http://www.sjst.psu.ac.th

Original Article

Microstructure and wear behavior of arc thermal sprayed base-cutter blades in sugarcane harvesters

Chuleeporn Paa-rai[1*], and Nuchira Dejang[2]

[1] *Department of Industrial Engineering, Faculty of Engineering, Naresuan University, Mueang, Phitsanulok, 65000 Thailand*

[2] *Department of Physics, Faculty of Science, Naresuan University, Mueang, Phitsanulok, 65000 Thailand*

Received: 20 November 2023; Revised: 13 March 2024; Accepted: 19 April 2024

Abstract

Base-cutter blades operate close to the soil during sugarcane harvesting, causing a high wear rate. The present study aims to improve the wear resistance of the blades with an economical surface treatment, so wire arc thermal spray was applied with two alternative types of cored wires, namely chrome nickel amorphous (AM) and titanium tungsten carbide (TiW). The microstructure study showed that AM coating contained an amorphous structure, while the TiW coating appeared to have a relatively non-homogeneous structure containing W and Ti carbide dispersion resulting in a higher hardness (876.40 $HV_{0.1}$) than that of AM coating (814.48 $HV_{0.1}$). However, after dry sand rubber testing, the AM coating exhibited nearly 2 times lower wear rate than that of the uncoated base-cutter blades or TiW coated ones. Therefore, the arc sprayed AM coating can be an economical approach to extend the service life of the blades.

Keywords: arc thermal spray, base-cutter blades of sugarcane harvester, chrome nickel amorphous, titanium tungsten carbide

1. Introduction

Base-cutter blades of sugarcane harvesters are applied to cut sugarcane adjacent to the ground, so they can hit stones and be abraded by sand or soil (Rodríguez, Duran, Aguilar, Alcázar, & Zambrano, 2020) causing rapid wear of the blades. Prolonging the service live of blades by increasing their wear resistance is a potential competitive advantage, which could reduce maintenance costs and off-service time during sugarcane harvest season.

Various thermal spray techniques have been applied to improve wear resistance of agricultural components. High-velocity oxygen fuel (HVOF)-sprayed WC/Co and plasma-sprayed Al_2O_3/NiAl coating on rotary tiller blades improved hardness of the blades, but only HVOF-sprayed WC/Co provided approximately 43 times greater wear resistance than that of the uncoated blades after testing in a sugarcane field including hard dry sandy soil (Karoonboonyanan, Salokhe, & Niranatlumpong, 2007). The arc sprayed WC-FeCrCoNiTi coating on cutter blades of sugarcane harvester could double the life time of the blades (Cooke, 2019). A study (Kang, Grewal, Jain, & Kang, 2012) found that D-Gun sprayed WC-Co-Cr coating on rotavator blades presented a lower wear rate than those with Cr_3C_2NiCr and Stellite-21 coatings, and significantly reduced wear rate compared to that of the uncoated blades. It is worth noting that the coatings, which have been shown to successfully improve the wear resistance of agricultural equipment, mostly consist of WC.

It has been known that Fe-based amorphous coatings have excellent corrosion and wear resistance despite the relatively inexpensive coating materials. A study (Milanti-Vuoristo *et al*., 2016) presented that HVOF and HVAF-sprayed Fe-Cr-Ni-Mo-Si-B-C coating gave a lower sliding wear rate than that with Fe-Cr-Ni-Si-B-C coating, due to a high nano-hardness related to inter-lamellar cohesive strength and large elasticity. Arc sprayed Fe-Cr-C-based coating on

*Corresponding author
Email address: chuleepornp@nu.ac.th

1020 steel showed wear and heat resistance in the range of 20 - 700 °C (Yury-Vuoristo *et al.,* 2018), and also, the coating with borides exhibited strengthening phases in abrasive wear. However, this type of coating on agricultural parts has been rarely studied.

The aim of this work was to improve the wear resistance of the base-cutter blades for sugarcane harvesters with an economical surface treatment process. Among many thermal spray techniques, an arc thermal spray is a cost-effective method giving good relative bond strength of coating (Sidhu, Prakash, & Agrawal, 2005), so this will be used with two alternative types of commercial core wires, namely chrome nickel amorphous and titanium tungsten carbide. The coated blades will be tested for their hardness and wear in relation to their microstructures.

2. Materials and Methods

2.1 Materials and coatings

Commercial base-cutter blades with 4 mm thickness and the chemical composition shown in Table 1 were studied in this research. They were cut into coupons of size 30 x 40 x 4 mm^3, then blasted with aluminum oxide grit (mesh #24) to prepare the surface roughness for wire arc thermal spraying.

Thermion Auto Arc AVD350 Arc Spray System with Jet Force Head Spray Gun was operated with two commercial Fe-based core wires, i.e. chrome nickel amorphous (30Cr10Ni10Nb4B2Al, for short AM), and titanium tungsten carbide (26WC13Cr6TiC6Ni2B1Si, for short TiW), both of 1.6 mm diameter, to create two types of coatings denoted by AM and TiW coatings, of 300 µm thickness. The wire arc parameters were 65 PSI air pressure and 100 A current for both types of core wires, but voltages were set at 30 V for TiW coating and 33 V for AM coating.

2.2 Wear testing

A dry sand rubber wheel designed under ASTM65 standard was applied to study the wear behavior of the samples with and without coatings. There were three replicate samples of each type of coating. In preliminary experiments, it was found that the load of 876 g with silicon sand of size 0.14-0.29 mm was appropriate for the test. The test coupons were measured for mass loss every 300 m and the wear test was finished when the distance reached 2,400 m. The mass loss versus distance was fit with a linear model having the wear rate as its slope:

$$\text{Wear rate} = \text{mass loss/distance} \quad (1)$$

2.3 Microstructural characterization and hardness testing

To examine the worn surface and the microstructure of the coatings of 300 µm thickness, Field Emission Scanning Electron Microscopy (FESEM) with Thermo Scientific Apreo 2 model was utilized. The coating compositions were analyzed by using energy-dispersive x-ray analysis (EDX) system in the FESEM, and X-ray diffraction (XRD) by D2Phaser Bruker (Detector: Lynxeye XE-T) was used to characterize the phases' chemical compositions in the coatings. The porosity and thickness of the coatings was measured using ImageJ analysis software on optical micrographs of cross-sections of the coatings. The hardness of each coating was measured using a Vickers microhardness tester (HVS-1000Z) with the load of 100 g and the dwell time of 15 s.

3. Results and Discussion

3.1 Microstructure characterization

The cross-sectional microstructures of AM and TiW coatings are shown in Figure 1 with the average thicknesses of 248.8±16.4 µm and 225.04±13.16 µm, respectively, determined by applying ImageJ software on 5 optical micrographs of the coatings, and measuring the thickness at 5 points of each micrograph. Some loss of coating thickness possibly happened during metallography sample preparation. However, both microstructures in Figure 1 contained wave-like lamellar structures, which is a general characteristic of thermal spray coatings, with porosities of 2.35% and 5.88% for the AM and TiW coatings, respectively. The microstructure can be divided into three areas, i.e. bright, dark and gray areas. In comparison, it is obvious that AM coating microstructure is relatively homogeneous. The elemental composition identified using EDX presented that most areas of the AM coating, shown as the gray area in Figure 1A, are Fe-enriched phase but also include Cr and Ni. The dark and bright spots, indicated by A and B in the image, are rich in Al and Nb phases, respectively, as seen from the EDX spectra for points A and B (Figure 2B). Considering the XRD pattern of the AM coating in Figure 2C, it is noticeable that the XRD pattern shows broad peaks associated with amorphous structure. However, a few very weak diffraction peaks could be related to cubic-Fe and hexagonal-NbFeB phases. This is consistent with the phase identification in Fe-Cr-Nb-B coating created by powder flame spraying and low velocity oxygen fuel processing (Koga-Botta *et al.*, 2014).

For the TiW coating, the XRD pattern in Figure 3C presents clear peaks related to crystalline phases including cubic-Ni-Cr-Fe, monoclinic-Fe_5C_2, cubic-FeSi, and tetragonal-Fe_2B phases. The cross-sectional microstructure of the coating shown in Figure 1B displays nonhomogeneous characteristic, and it was discovered that the main gray area consisted of Fe, Cr and Ni, according to the elemental mapping in Figure 3A. The dark areas, such as C point in Figure 1B, showed high contents of Ti and C as displayed in the elemental mapping (Figure 3A) and the EDX spectrum in Figure 3B. For the bright area marked by D in Figure 1B, it was found to have a high concentration of W; see also the

Table 1. Chemical composition of base-cutter blades for sugarcane (wt.%)

C	Mn	Si	Cr	Ni	Sn	Ti	Al	S	P	Other	Fe
0.346	0.183	0.107	0.074	0.057	0.048	0.038	0.032	0.018	0.008	0.177	Bal.

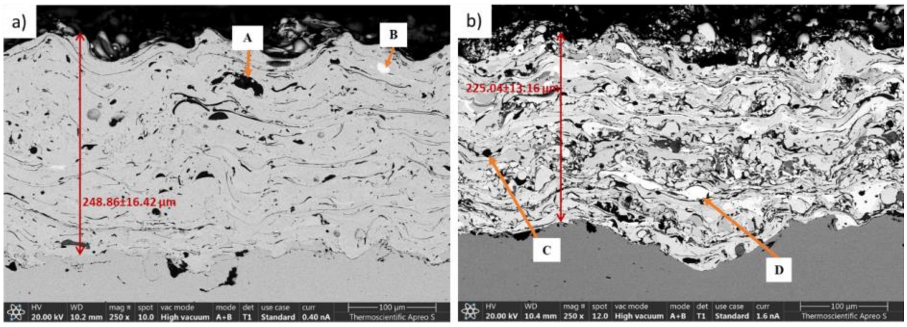

Figure 1. SEM micrographs of a) AM, and b) TiW coating microstructures

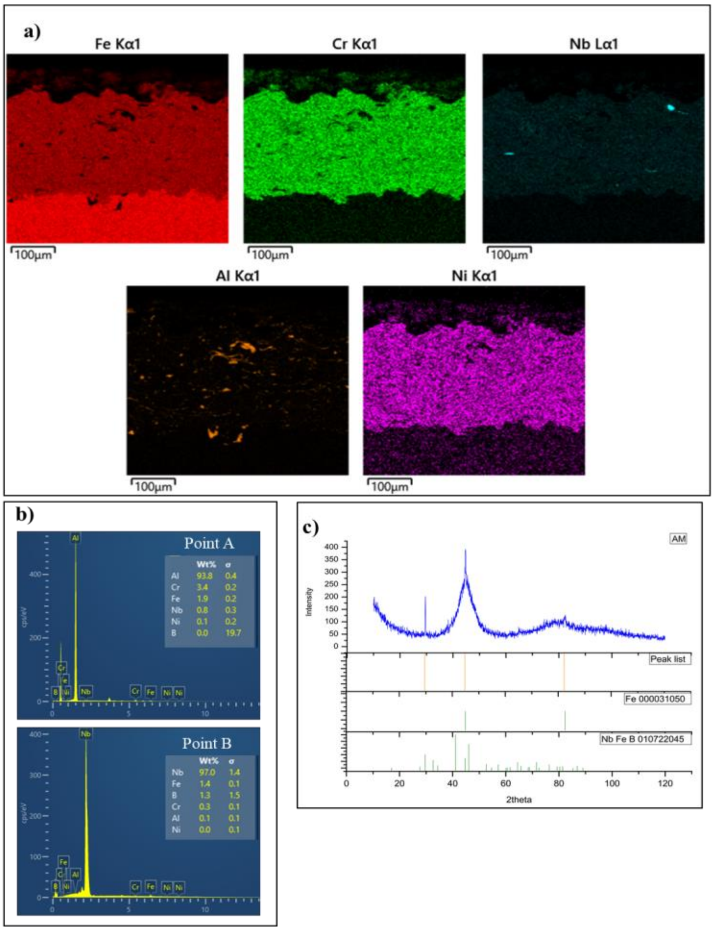

Figure 2. EDX analysis and XRD plot of AM coating: a) elemental mapping of the area of Figure 1A, b) EDX spectra of points A and B in Figure 1A, and c) XRD plot of AM coating

elemental mapping in Figure 3A and the EDX spectrum in Figure 3B. This might be attributed to the WC, which is the second main component of the core wire used for TiW coating.

Both as-sprayed AM and TiW coatings were observed for their top surfaces, displayed in Figure 4A and 4B, respectively. Some unmelted particles of round shape on the surface of TiW coating and also some cracks (marked with circles), which might be caused by different thermal shrinkage during the cooling of the various phases in the microstructure, are evident. In contrast, no cracks were observed on the surface of the AM coating (Figure 4A).

3.2 Wear behavior of coatings

Figure 5 presents a plot of cumulative mass losses of uncoated base-cutter, and TiW and AM coatings vs. the distance. Fluctuations in mass loss can be noted from the beginning to 1200 m. This can be considered the run-in period (Zambrano, Muñoz, Rodríguez, & Coronado, 2020). It is

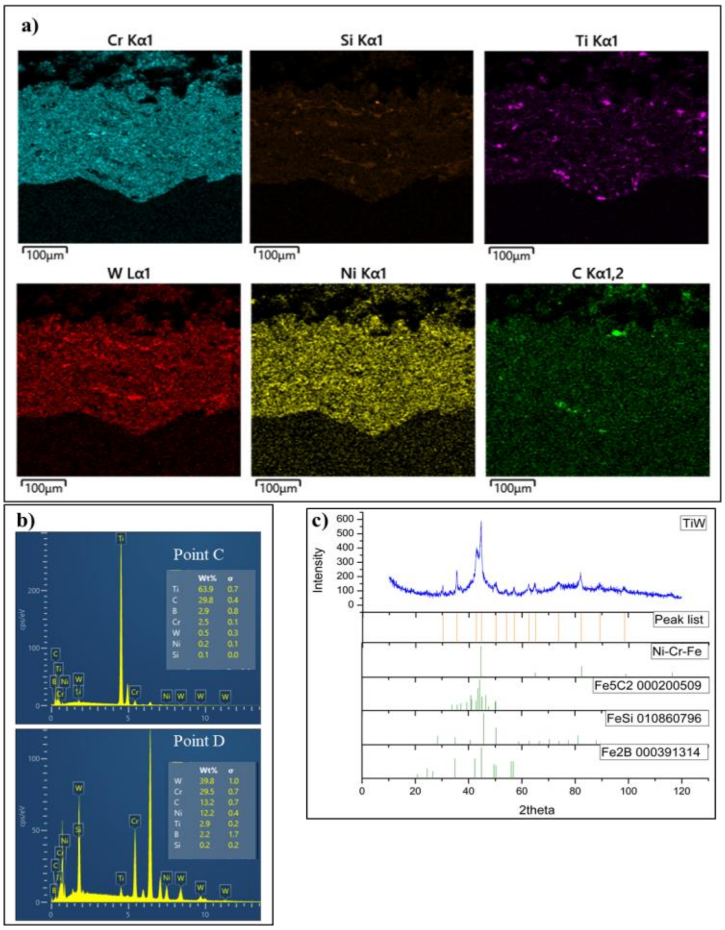

Figure 3. EDX analysis and XRD plot of TiW coating: a) elemental mapping of the area of Figure 1B, b) EDX spectra of points C and D in Figure 1B, and c) XRD plot of TiW coating.

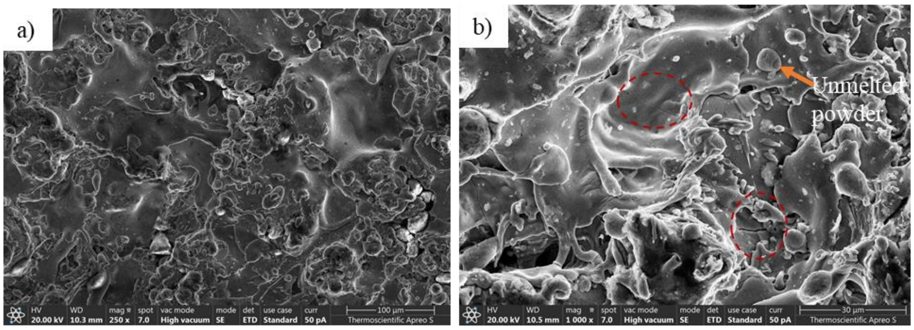

Figure 4. Electron micrographs of the top surfaces of as-sprayed a) AM, and b) TiW coatings.

obvious that the uncoated blade exhibited higher mass loss than its coated counterparts. The wear rates were determined as slopes of linear fits, and are presented with hardness results in Figure 6. It can be seen that AM coating provided significant reduction in wear rate, 0.024 mg/m, as compared to the uncoated blades, 0.039 mg/m, which was similar to that with the TiW coating, 0.032 mg/m. Both coatings provide about twofold greater hardness than that of the uncoated sample (439.10 $HV_{0.1}$), whilst TiW coating hardness (876.40 $HV_{0.1}$) is slightly higher than that of AM coating (814.475 $HV_{0.1}$).

The AM and TiW coating surfaces after the abrasive wear testing were examined using SEM, see Figures 7 and 8, respectively. The damaged surfaces of both coatings show some abrasive grooves and delamination. This agrees with prior studies of wear surface morphology of Fe-based and amorphous thermal spray coatings (Bolelli-Vuoristo *et al*., 2016; He, Fu, Jiang, & Li, 2008; Priyan & Hariharan, 2012; Zhou, Wang, He, Wang, & Liu, 2010). Considering in detail of the worn surfaces shown in Figure 7B and 8B, it is obvious that the morphology of the scar wear on both coatings showed some deformation and small cracks, for example, the indexed

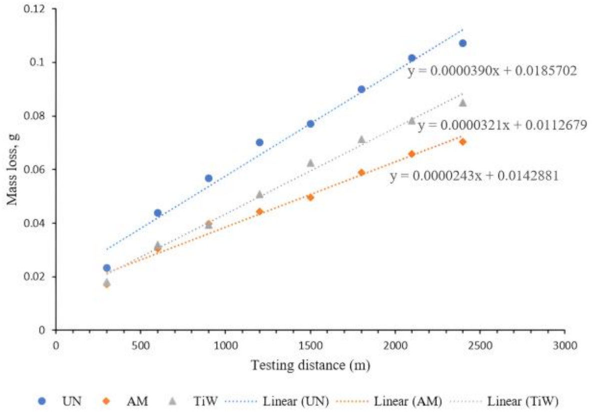

Figure 5. Cumulative mass loss during dry sand rubber wheel test for uncoated base-cutter blade for sugarcane, and blades with AM and TiW coatings

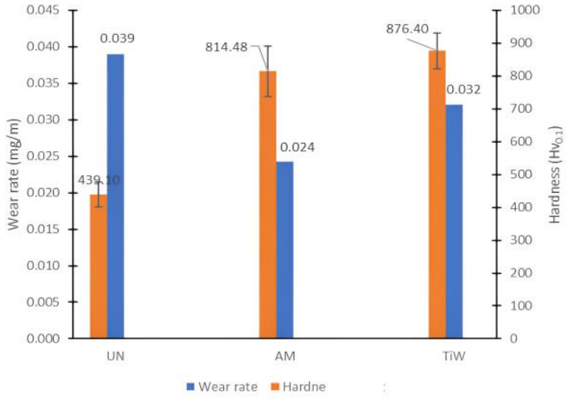

Figure 6. Hardness and relative wear resistance for uncoated base-cutter blade for sugarcane, and blades with AM and TiW coatings

circles in Figure 7B and 8B. This results from high-stress abrasion grinding and fatigue load (Yuan-Yang *et al*., 2022) during the dry sand rubber wheel testing. After the micro-cracks have been created under the fatigue load, some of coating surfaces will fall off resulting in debris.

An examination of cross-section of worn surface provided the chemical composition details of AM and TiW cases, displayed in Figures 9 and 10, respectively. The main area of the AM coating exhibited as light gray area containing high amount of Fe (2-spectrum in Figure 9). Some delamination of the coating was found with high oxygen concentration as shown in 1-spectrum in Figure 9. The AM worn surface revealed less damage in comparison than the TiW warn surface, displayed in Figure 10. Cracks and fractures were observed in the light gray areas of the microstructure containing high concentration of Fe (1, 4 and 5 spectra in Figure 10). Also, the chemical composition of some debris was examined. The results (2 and 3 spectrums in Figure 10) indicate that they could be Ti carbide and Ti oxide phases. This supports the explanation of the wear mechanism in other works (He *et al.*, 2008; Murthy & Venkataraman, 2006; Sudaprasert, Shipway, & McCartney, 2003) in that the coating with carbides started wearing by locally removing of the soft area surrounding the carbides due to plastic deformation and fatigue, caused by continual attacks by the abrasive particles, and then undercutting of the carbide particles. The debris could also have other abrasive particles from the wear process causing severe damage to the coating. Those cracks in soft Fe

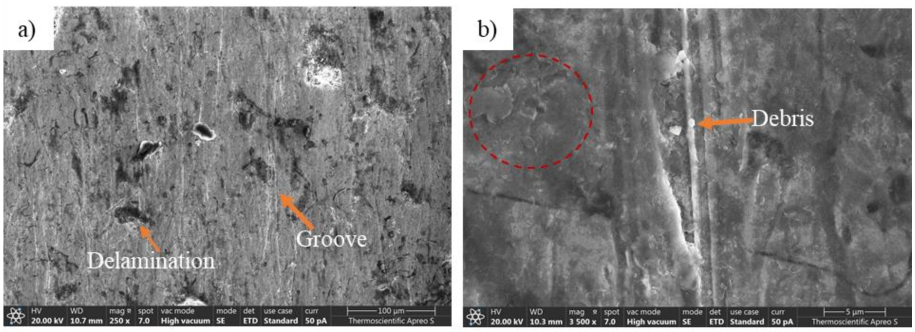

Figure 7. Electron micrographs of worn surfaces of AM coatings: a) overview, and b) detail of a groove

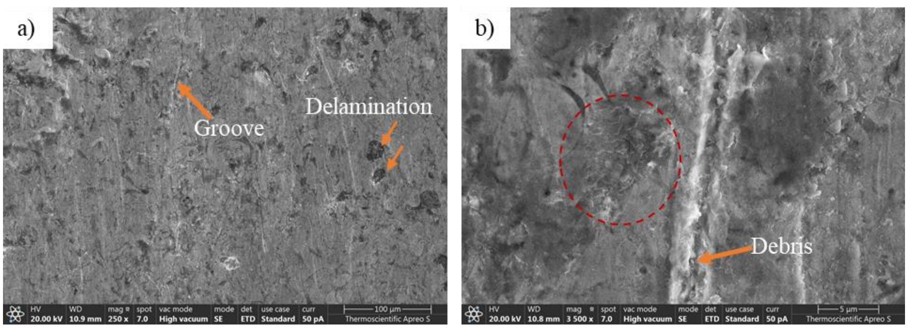

Figure 8. Electron micrographs of worn surfaces of TiW coatings: a) overview, and b) detail of a groove

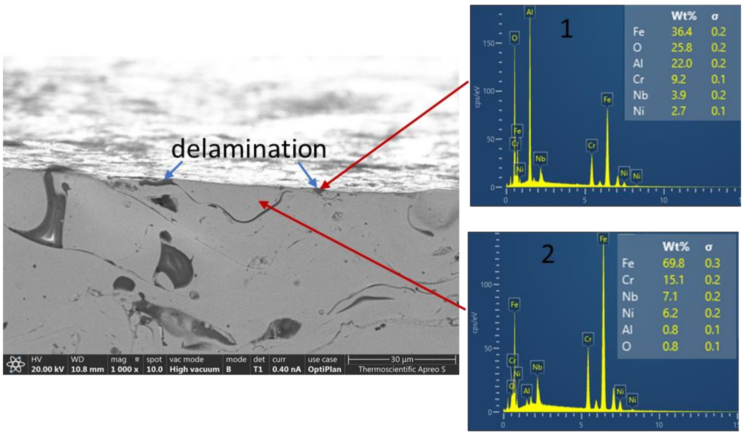

Figure 9. Electron micrographs of cross-sectional worn surfaces of AM coating with EDX spectra

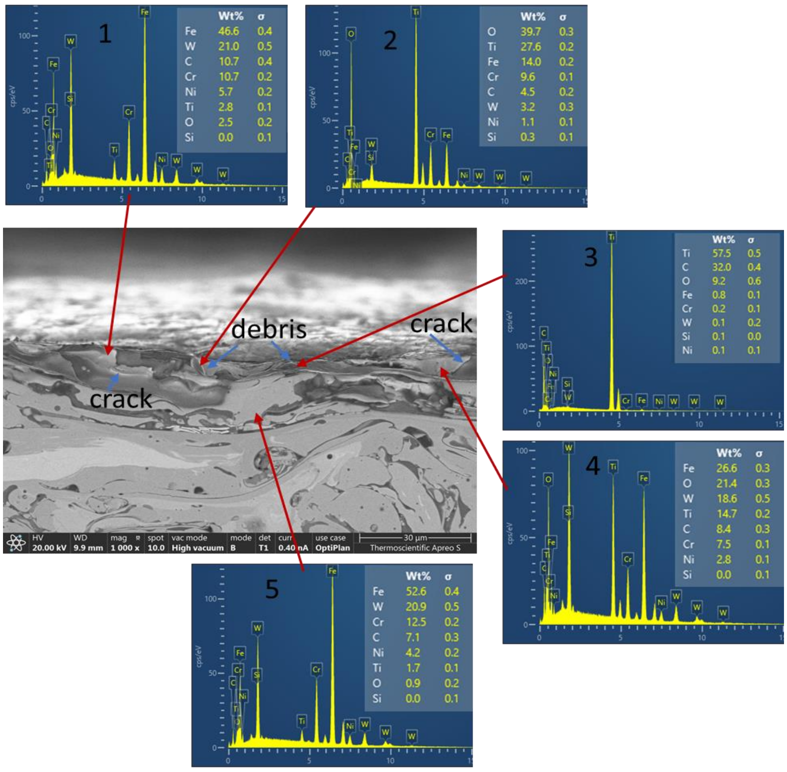

Figure 10. Electron micrographs of cross-sectional worn surfaces of TiW coating with EDX spectra

rich areas subsequently caused the hard carbide and oxide particles to fall off and became abrasive particles in the wear testing. This provided more damage and more mass loss to the TiW coating over the AM coating. Also, the micro-cracks observed on as-sprayed surface of TiW, marked by circles in Figure 4B, might be another reason for the high wear rate of the coating.

4. Conclusions

The arc wire thermal spray coatings of chrome nickel amorphous (AM) and titanium tungsten carbide (TiW) on base-cutter blades were studied and the results can be summarized as follows:

• The microstructure of AM coating was more homogenous than that of TiW coating that was found to contain hard phases such as W and Ti carbides. This resulted in the higher hardness of TiW coating, but it had the larger wear mass loss.

• The wear rates of TiW and AM coatings were 0.032 and 0.024 mg/m, respectively, while the uncoated blade presented 0.039 mg/m ware rate.

• The AM coating produced by wire arc spray process is capable of extending the service life of the base-cutter blades for sugarcane harvesters without adding too much to the production cost of blades.

Acknowledgements

This work was supported by Naresuan University, National Science, Research and Innovation Fund (NSRF) Grant number R2565B065.

References

Bolelli, G., Milanti, A., Lusvarghi, L., Trombi, L., Koivuluoto, H., & Vuoristo, P. (2016). Wear and impact behaviour of high velocity air-fuel sprayed Fe-Cr-Ni-B-C alloy coatings. *Tribology International*, *95*, 372–390. Retrieved from https://doi.org/10.1016/j.triboint.2015.11.036

Cook, K. O. (2019). Thermally sprayed coatings for increased wear resistance of cutting blades used in harvesting sugarcane. *Annals of Agricultural and Crop Sciences*, *4*(1), 1–7.

He, D. Y., Fu, B. Y., Jiang, J. M., & Li, X. Y. (2008). Microstructure and wear performance of arc sprayed Fe-FeB-WC coatings. *Journal of Thermal Spray Technology*, *17*(5–6), 757–761. Retrieved from https://doi.org/10.1007/s11666-008-9257-2

Kang, A. S., Grewal, J. S., Jain, D., & Kang, S. (2012). Wear behavior of thermal spray coatings on rotavator blades. *Journal of Thermal Spray Technology*, *21*(2), 355–359. Retrieved from https://doi.org/10.1007/s11666-011-9709-y

Karoonboonyanan, S., Salokhe, V. M., & Niranatlumpong, P. (2007). Wear resistance of thermally sprayed rotary tiller blades. *Wear*, *263*, 604–608. doi:10.1016/j.wear.2006.12.072

Koga, G. Y., Nogueira, R. P., Roche, V., Yavari, A. R., Melle, A. K., Gallego, J., . . . Botta, W. J. (2014). Corrosion properties of Fe-Cr-Nb-B amorphous alloys and coatings. *Surface and Coatings Technology*, *254*, 238–243. Retrieved from https://doi.org/10.1016/j.surfcoat.2014.06.022

Milanti, A., Matikainen, V., Bolelli, G., Koivuluoto, H., Lusvarghi, L., & Vuoristo, P. (2016). Microstructure and sliding wear behavior of Fe-based coatings manufactured with HVOF and HVAF thermal spray processes. *Journal of Thermal Spray Technology*, *25*(5), 1040–1055. Retrieved from https://doi.org/10.1007/s11666-016-0410-z

Murthy, J. K. N., & Venkataraman, B. (2006). Abrasive wear behaviour of WC–CoCr and Cr3C2–20(NiCr) deposited by HVOF and detonation spray processes. *Surface and Coatings Technology*, *200*(8), 2642–2652. Retrieved from https://doi.org/10.1016/J.SURFCOAT.2004.10.136

Priyan, M. S., & Hariharan, P. (2012). The study on tribology and surface interface characterization of FE based alloy coating deposited by HVOF method. *Procedia Engineering*, *38*, 3741–3756. Retrieved from https://doi.org/10.1016/j.proeng.2012.06.430

Rodríguez, J. S., Duran, J. F., Aguilar, Y., Alcázar, G. A. P., & Zambrano, O. A. (2020). Failure analysis in sugar cane cutter base blades. *Engineering Failure Analysis*, *112*. Retrieved from https://doi.org/10.1016/j.engfailanal.2020.104503

Sidhu, T. S., Prakash, S., & Agrawal, R. D. (2005). Studies on the properties of high-velocity oxy-fuel thermal spray coatings for higher temperature applications. *Materials Science*, *41*(6), 805–823. Retrieved from https://doi.org/10.1007/s11003-006-0047-z

Sudaprasert, T., Shipway, P. H., & McCartney, D. G. (2003). Sliding wear behaviour of HVOF sprayed WC–Co coatings deposited with both gas-fuelled and liquid-fuelled systems. *Wear*, *255*(7–12), 943–949. Retrieved from https://doi.org/10.1016/S0043-1648(03)00293-X

Yuan, W., Wang, H., Guo, Q., Wang, W., Zhu, Y., Yu, J., & Yang, X. (2022). Study on wear mechanism of helical gear by three-body abrasive based on impact load. *Materials*, *15*(12), 4135. Retrieved from https://doi.org/10.3390/ma15124135

Yury, K., Filippov, M., Makarov, A., Malygina, I., Soboleva, N., Fantozzi, D., . . . Vuoristo, P. (2018). Arc-sprayed Fe-based coatings from coredwires for wear and corrosion protection in power engineering. *Coatings*, *8*(2), 71. Retrieved from https://doi.org/10.3390/coatings8020071

Zambrano, O. A., Muñoz, E. C., Rodríguez, S. A., & Coronado, J. J. (2020). Running-in period for the abrasive wear of austenitic steels. *Wear*, 452–453. Retrieved from https://doi.org/10.1016/j.wear.2020.203298

Zhou, Z., Wang, L., He, D. Y., Wang, F. C., & Liu, Y. B. (2010). Microstructure and wear resistance of Fe-based amorphous metallic coatings prepared by HVOF thermal spraying. *Journal of Thermal Spray Technology*, *19*(6), 1287–1293. Retrieved from https://doi.org/10.1007/s11666-010-9556-2